

17th International Symposium on District Heating and Cooling, September 2021, Nottingham, UK

Comparison of discrete dynamic pipeline models for operational optimization of District Heating Networks

Jona Maurer*, Oliver M. Ratzel, Albertus J. Malan, Sören Hohmann

Institute of Control Systems, Karlsruhe Institute of Technology, Wilhelm-Jordan-Weg 1, 76131 Karlsruhe, Germany

Received 11 August 2021; accepted 22 August 2021

Abstract

Optimal operation of District Heating Networks (DHNs) is a very challenging task. One of the main challenges for DHNs optimization tool designers is the choice of an adequate dynamic thermal pipeline model which gives a good tradeoff between accurately modeling the physics of the thermodynamic processes and simultaneously yielding a numerically efficient model. To address this, the paper states the main Partial Differential Equation (PDE) which is used to describe the convection of hot water throughout the literature, together with reasonable assumptions that lead to minor deviations from measurements. Then, different approaches are described which can be used to solve the respective PDE. More specifically, the very common Node Method (NM), approximations of the NM, the lagrangian approach and different Finite Difference (FD) approaches are presented. The main aim of this work is to provide a qualitative and quantitative comparison of these modeling approaches in the context of optimal DHN operation. Our quantitative results show, that by comparing the different approaches to measurement data, the NM yields the smallest modeling errors for most of the temporal discretization sizes. The qualitative comparison identifies that the lagrangian method lacks the differentiability necessary for the implementation in optimization tools. The advantages of the FD approaches include guaranteeing a fixed number of variables, a constant information depth of the temperature distribution along the pipeline and the simplicity of implementation into optimization tools. The approximations of the NM bring benefits when varying mass flow directions need to be considered, which is a crucial aspect in 4th generation DHNs.

© 2021 The Author(s). Published by Elsevier Ltd. This is an open access article under the CC BY-NC-ND license (<http://creativecommons.org/licenses/by-nc-nd/4.0/>).

Peer-review under responsibility of the scientific committee of the 17th International Symposium on District Heating and Cooling, 2021.

Keywords: Modeling; Pipeline; Optimal operation of DHNs

1. Introduction

District Heating Networks (DHNs) will be a key technology for a successful energy transition [1,2]. Thereby, the optimal operation of DHNs is a major task to reduce losses, save costs [3], lower emissions [4] or obtain an optimal interaction of DHNs and electric power systems [5,6], to e.g. reduce the need for grid reinforcements. The basis of optimal operation of a DHN is an optimization problem which usually incorporates a model of the respective DHN.

* Corresponding author.

E-mail address: jona.maurer@kit.edu (J. Maurer).

<https://doi.org/10.1016/j.egy.2021.08.150>

2352-4847/© 2021 The Author(s). Published by Elsevier Ltd. This is an open access article under the CC BY-NC-ND license (<http://creativecommons.org/licenses/by-nc-nd/4.0/>).

Peer-review under responsibility of the scientific committee of the 17th International Symposium on District Heating and Cooling, 2021.

Nomenclature

CFL	Courant–Friedrichs–Lewy
DHN	District Heating Network
DQ	Difference Quotients
EM	Element Method
FD	Finite Difference
FEM	Finite Element Model
FV	Finite Volume
MC	Method of Characteristics
MINLP	Mixed Integer Nonlinear Programming
NLP	Nonlinear Programming
NM	Node Method
PDE	Partial Differential Equation
RMSE	Root Mean Square Error
A	cross-section area
c	specific heat capacity
c_{st}	specific heat capacity of steel
c_w	specific heat capacity of water
C_{ws}	combined heat capacity of steel and water
d_1	inner diameter
d_2	outer diameter
I	number of sampling points in space
Δk	time span of a time step
k_h	heat transmission coefficient
L	pipe length
\dot{m}	mass flow
N	number of sampling points in time
R	water mass
S	water mass
t	time
Δt	time step width
t_{stay}	average length of stay of the water masses leaving the pipeline
T	temperature
T_a	ambient temperature
T_i	temperature of water mass i
T_i^n	temperature at space x_i and time t_n
$T_{out,1}$	lossless output temperature
$T_{out,2}$	output temperature
T_{st}	temperature of the steel core
x	space
Δx	spatial step
γ	auxiliary variable
ε	auxiliary variable
κ_w	thermal conductivity of water

ρ	density
ρ_{st}	density of steel
ρ_w	density of water

Typically, a DHN model is divided into a hydraulic and a thermal model. The hydraulic model is used to calculate the mass flows and pressure losses in the individual DHN components. The mass flows are used by the thermal model to calculate the temperatures at outputs, inputs and throughout the pipelines. The most common components in DHNs are pipelines. As, on the one hand, imprecise pipeline models lead to significant subsequent errors and, on the other hand, overly complex models result in very large, often nonlinear, optimization problems which are not solvable in real time, an accurate model choice is of profound interest. In contrast to simulation, the models applied in operational optimization need to be differentiable to enable real-time optimization. This requirement limits the viability of well-known simulation models for operational optimization. However, as presented in detail later in the introduction, there is very little literature comparing these different dynamic pipeline models for operational optimization of DHNs, which is why this work aims to bridge that gap.

Note that apart from pipelines, the thermal and hydraulic models of DHN components, e.g. pumps, valves, producers, consumers and nodes, typically contain nonlinearities, as e.g. in [7]. Therefore, the entire optimization problem usually results in a Nonlinear Programming (NLP) or a Mixed Integer Nonlinear Programming (MINLP) problem. DHN pipelines can be described by dynamic or stationary models [8]. As dynamic models more accurately represent the underlying physics, they will be studied in detail here. In optimization problems, discrete dynamic problems lead to stationary optimization problems which do not have to solve the discretization problem at runtime, while still representing the dynamic effects of the underlying physics [9]. This is a valuable aspect considering the already high computational burden of optimal operation of DHNs [10]. Furthermore, discrete pipeline models can easily be aligned with discrete measurement data and discrete bids in the context of market-based control of DHNs [4,11,12]. Hence, in this paper different dynamic, discrete, thermal pipeline models are compared quantitatively and qualitatively.

The Partial Differential Equation (PDE) describing the convection of heat in a DHN pipeline can be derived from the first law of thermodynamics for open systems [13]:

$$\underbrace{\rho_w c_w A \frac{\partial T}{\partial t}}_1 + \underbrace{\dot{m} c_w \frac{\partial T}{\partial x}}_2 = \underbrace{\kappa_w A \frac{\partial^2 T}{\partial x^2}}_3 + \underbrace{k_h (T_a - T)}_4 \quad (1)$$

Herein ρ_w denotes the density of water, c_w the specific heat capacity of water, A the cross sectional area of the pipeline, T the temperature of the water, ∂t the temporal and ∂x the spatial change, \dot{m} the mass flow, κ_w the thermal conductivity of water, k_h the heat transmission coefficient and T_a the ambient temperature.

The four terms of the PDE in (1) are: (1) the change due to internal energy, (2) the enthalpy flux of water, (3) the conductive heat transfer in the fluid, and 4) the convective heat transmission through the insulation of the pipeline [13]. This PDE is based on the following assumptions commonly found throughout the literature [7,13–16]: (i) The transport medium is incompressible and has a constant density ρ and a specific heat capacity c ; (ii) Frictional heat is negligible, the pipeline is cylindrical, has a constant heat transmission coefficient and the ambient temperature is constant along the length of the pipeline; (iii) The cross-section of a pipeline has spatially homogeneous velocity and temperature throughout [7], and heat diffusion in the axial direction is neglected [16], leading to the simplified PDE, as follows:

$$\rho_w c_w A \frac{\partial T}{\partial t} + \dot{m} c_w \frac{\partial T}{\partial x} = k_h (T_a - T) \quad (2)$$

These assumptions bring great benefit as they allow a one-dimensional spatial model of the pipeline while leading to accurate approximations as shown in Section 4.

There are several approaches used to solve the PDE in (2) [15,17–19]. The so-called Node Method (NM) was introduced in [15] and compared with the Element Method (EM), a Finite Difference (FD) approach. In [18], an FD approach was compared to the NM but the effects of temperature losses through the insulation and the steel core of the pipeline were neglected. The authors of [17] compared five different explicit FD approaches but did not

consider implicit approaches which are unconditionally stable. A comparison of the implicit upwind method and the Method of Characteristics (MC) model was performed in [19] and recommended time and spatial step sizes were stated. An approach based on the MC is presented and compared to the NM and Finite Volume (FV) approaches in [20]. In comparison to [15] and [18], the developed model distinguishes between the turbulent core and the boundary layers of the water mass to achieve higher modeling accuracy for simulation purposes. This higher level of modeling accuracy necessitates additional parameters and increases the computational burden, and is therefore not further considered here. In [21] a Finite Element Model (FEM) was proposed and compared to the EM and the NM. The NM and the FEM are validated against measurement data with a very small temperature gradient of 5°C/2 h. Furthermore, only two different spatial step lengths are compared at a fixed small time-step length.

A second group of papers gives a broad overview of the optimization of DHNs [22–24]. In [22], published models of DHNs are classified as either deterministic or stochastic energy models and existing software recommendations for the respective implementations are stated. In [23], several models for different DHN components can be found. The authors of [24] present different optimization techniques applied to DHN optimization but omit the aspect of pipeline modeling. Nevertheless, none of these papers consider pipeline models in a detailed methodical form.

As none of the papers above has given a full quantitative and qualitative comparison of the different FD approaches, the FV approach and the different forms of the NM, we aim to bridge that gap by facilitating the choice of an adequate thermal pipeline model for future DHN optimization tool designers.

The rest of this paper is structured as follows. Section 2 describes different methods to solve the PDE (2). The test setup and simulation environment used to carry out the quantitative comparison is described in Section 3. The results of the quantitative and qualitative comparison are depicted in Section 4. Finally, the main contributions are highlighted in Section 5.

2. Methods for solving the partial differential equation

Two main groups of methods to solve the PDE (2) are presented in this section. The first is the MC, resulting in the NM, and the second is the group of the FD approaches. In the one-dimensional case, with fixed intersection and equidistant spatial discretization, the FV and FD approaches become identical [25]. Thus, FV approaches are not further regarded here.

2.1. Method of characteristics – The node method

The MC uses a transformation of the PDE into a new set of coordinates to describe the solution of the PDE on characteristics with a reduced set of coordinates, depending on its initial conditions [26]. This model was first introduced in [15], where it is presented in the following discretized form and called the NM, as temperatures are only calculated at the outlet of a pipeline based on the input temperatures of the previous steps. The outlet temperature of a pipeline $T_{out,2}$ is among others dependent on the lossless output temperature $T_{out,1}$ and the time step k .

$$T_{out,2}(k) = T_a(k) + (T_{out,1}(k) - T_a(k)) \exp\left(-\frac{k_h t_{stay}(k)}{\rho_w c_w A}\right) \quad (3)$$

The lossless outlet temperature $T_{out,1}$ is calculated by a weighted sum of the temperatures T_i of the water masses that have entered the pipeline in the previous several time steps.

$$T_{out,1}(k) = \frac{1}{\dot{m}(k)\Delta k} [(R(k) - \rho_w AL) T_i(k - \gamma(k)) + \sum_{\kappa=k-\varepsilon(k)+1}^{k-\gamma(k)-1} (\dot{m}(\kappa)\Delta k T_i(\kappa)) + (\dot{m}(k)\Delta k + \rho_w AL - S(k)) T_i(k - \varepsilon(k))] \quad (4)$$

The three parts of the weighted mass, see Fig. 1, are described by the auxiliary variables, γ and ε and the water masses R and S , which can be calculated as in [15]. Thereby, γ and ε describe the time step at which the water mass entered the pipeline which is now the last (γ) and respectively the first to leave the pipeline (ε). With these auxiliary time steps the auxiliary water masses R and S , see Fig. 1, can be calculated.

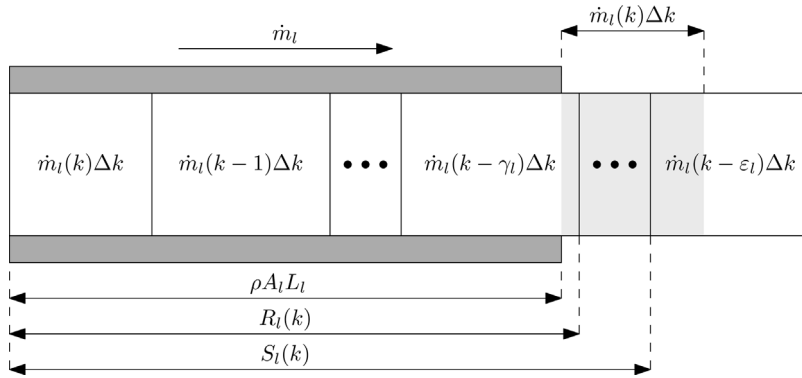


Fig. 1. Scheme of a pipeline and the relevant variables of the NM.

The entire water mass in the pipeline is calculated by the product of the density of water ρ_w , the cross-section area A , and length L of the pipeline. The time span of a time step Δk is then used together with the currently inflowing mass flow $\dot{m}(k)$ to define the total amount of water mass leaving the pipeline at the respective time step. The average length of stay of the water masses leaving the pipeline t_{stay} is calculated by a weighted sum similar to the one in (4). This form, being more accurate but still computationally fast, was first introduced in [6] and is stated in (5) below:

$$t_{\text{stay}}(k) = \frac{1}{\dot{m}(k)\Delta k} [\gamma(k) (R(k) - \rho_w AL) + \sum_{\kappa=k-\varepsilon(k)+1}^{k-\gamma(k)-1} ((k - \kappa)\dot{m}(\kappa)\Delta k) + \varepsilon(k) (\dot{m}(k)\Delta k + \rho_w AL - S(k))] \Delta k \quad (5)$$

To calculate the outlet temperature of the pipeline while accounting for the low pass characteristic of the steel core of the pipeline $T_{\text{out},1, \text{st}}$ the formula (6) is introduced in [15] as follows:

$$T_{\text{out},1, \text{st}}(k) = \frac{T_{\text{out},1}(k)\dot{m}(k)c_w \Delta k + C_{st} T_{st}(k - 1)}{C_{st} + \dot{m}(k)c_w \Delta k}, \quad (6)$$

with the temperature of the steel core at the last time step $T_{st}(k - 1)$, which is determined by $T_{\text{out},1, \text{st}}$ of the last time step, so $T_{st}(k - 1) = T_{\text{out},1, \text{st}}(k - 1)$. The heat capacity of the entire steel core C_{st} of the pipe is calculated by:

$$C_{st} = \frac{\pi}{4} (d_2^2 - d_1^2) \rho_{st} c_{st} L, \quad (7)$$

with the inner and outer diameters d_1 and d_2 , the specific heat capacity c_{st} and density ρ_{st} of steel. If the steel core is considered, the final outlet temperature of the pipeline $T_{\text{out},2}$ is calculated by replacing $T_{\text{out},1}$ in Eq. (3) with $T_{\text{out},1, \text{st}}$.

2.2. The approximated node method

The auxiliary variables γ and ε used in (4)–(5) lead to an MINLP problem which is very time consuming to solve. To overcome this disadvantage, an adequate approximation is presented in our previous work [27] which leads to an NLP problem with a reduced computational burden. This model is used in a model predictive control context and uses mass flow approximations from the last time steps and measurement data. As the mass flow of the measurement used for validation and comparison of the different models in this work are constant, the results of the approximated NM are identical to the ones of the original NM, so it will not be further regarded here. Nevertheless, our comparison of this approximation with the original node method has shown almost the same accuracy while preventing the high computational burden, in previous case studies [27].

2.3. The Lagrangian approach

In [14] and [7], an approach is presented which can be seen as an extension of the NM. This approach seeks to increase the model accuracy of the thermal pipeline model by defining the temperature throughout the water masses using a linear interpolation of the temperature at the ends of each water mass. Instead of continuously merging multiple water masses at the end of a pipeline, as defined in (4) and visualized in Fig. 1, the water masses leaving a pipeline in one time step are handed to the next pipeline unmodified. A disadvantage of this approach is that this model leads to a non-differentiable model as different cases need to be checked, e.g. if a water mass has already entered a new pipeline or not. Therefore, it is a valid model for simulation with predefined input parameters in a DHN, but not easily utilizable for the real-time operational optimization in large DHNs and thus not further examined here.

2.4. Finite difference methods

With FD methods, the solution of a PDE, here (2), is calculated at discrete sampling points, in this context typically of space and time, by approximating the derivatives of the PDE by Difference Quotients (DQs). For (2), it is possible to represent the discretized space in a space–time plane (x, t) , where the spaces are considered on a one-dimensional axis. The spatial step width Δx and time step width Δt are chosen equidistant for the entire relevant space. In the following, the indices i and n are used for space x_i and time step t_n respectively. The shorthand T_i^n is used for $T(x_i, t_n)$.

The order of the selected DQ influences the order of the scheme. Depending on the chosen DQ, the approaches can be differentiated into explicit and implicit FD methods. Explicit approaches use a right-sided DQ, while implicit approaches use a left-sided DQ, for the approximation of the partial temporal derivative. To guarantee numerical stability, explicit approaches need to fulfill the Courant–Friedrichs–Lewy (CFL) condition [28]. An intuitive explanation of this condition is that the flow velocity has to be smaller than the propagation speed of the numeric calculation $\Delta x/\Delta t$ [19]. As the maximal flow velocity in DHNs of about 3 m/s leads to a high number of optimization variables, due to a need of closely spaced sampling points in space or/and time for each pipeline, only implicit FD approaches are considered here, which do not inherently impose a condition on the choice of the sampling points.

To consider the steel core of the pipeline, (2) can be transformed to:

$$C_{ws} \frac{\partial T}{\partial t} + \Delta x \dot{m} c_w \frac{\partial T}{\partial x} = \Delta x k_h (T_a - T), \quad C_{ws} = \Delta x \frac{\pi}{4} (\rho_w c_w d_1^2 + \rho_{st} c_{st} (d_2^2 - d_1^2)), \quad (8)$$

with the combined heat capacity of water and steel defined by C_{ws} , thereby assuming that the steel core and water in the respective space have the same temperature. This assumption is valid for small Δx due to the fact that “heat transfer between the water and the steel pipe as well as the heat conduction through the steel is very large compared to the heat transmission through the insulation and the ground” [15].

Various computational implementations of (8) are given in the following subsections.

2.4.1. Implicit upwind scheme

This scheme has the order $\mathcal{O}(\Delta x, \Delta t)$, i.e. first order difference quotients are used to approximate the partial spatial and temporal derivatives. Heat losses are accounted for by considering the temperature T at time step $n + 1$. The resulting implicit upwind scheme for (8) is shown below:

$$\left(\frac{C_{ws}}{\Delta t} + \dot{m} c_w + k_h \Delta x \right) T_i^{n+1} - \dot{m} c_w T_{i-1}^{n+1} = \frac{C_{ws}}{\Delta t} T_i^n + k_h \Delta x T_a \quad (9)$$

2.4.2. Full implicit scheme

This scheme has the order $\mathcal{O}(\Delta x^2, \Delta t)$. The spatial derivative is approximated by the following central difference quotient. The resulting full implicit scheme for (8) is shown below:

$$\frac{\dot{m} c_w}{2} T_{i+1}^{n+1} + \left(\frac{C_{ws}}{\Delta t} + k_h \Delta x \right) T_i^{n+1} - \frac{\dot{m} c_w}{2} T_{i-1}^{n+1} = \frac{C_{ws}}{\Delta t} T_i^n + k_h \Delta x T_a \quad (10)$$

2.4.3. Crank–Nicolson scheme

The order of this scheme is $\mathcal{O}(\Delta x^2, \Delta t^2)$. In this scheme, the values of the solution function at time step $n + 1/2$ are considered. The approximation of the local derivative is shown in (11), while accounting for the interpolation [28].

$$\frac{\partial T}{\partial x} = \frac{T_{i+1}^{n+1/2} - T_{i-1}^{n+1/2}}{2\Delta x} = \frac{T_{i+1}^{n+1} - T_{i-1}^{n+1} + T_{i+1}^n - T_{i-1}^n}{4\Delta x} \quad (11)$$

Heat losses are calculated based on the temperature T at time step $n + 1/2$. Thus, the right side of (8) can be formulated as:

$$\Delta x k_h (T_a - T(x, t)) \approx \Delta x k_h (T_a - T_i^{n+1/2}) = \Delta x k_h \left(T_a - \frac{1}{2}(T_i^{n+1} + T_i^n) \right) \quad (12)$$

The final equation for the scheme is given below:

$$\frac{\dot{m}c_w}{4} T_{i+1}^{n+1} + \left(\frac{C_{ws}}{\Delta t} + \frac{k_h \Delta x}{2} \right) T_i^{n+1} - \frac{\dot{m}c_w}{4} T_{i-1}^{n+1} = \left(\frac{C_{ws}}{\Delta t} - \frac{k_h \Delta x}{2} \right) T_i^n + k_h \Delta x T_a + \frac{\dot{m}c_w}{4} (T_{i-1}^n - T_{i+1}^n) \quad (13)$$

2.4.4. Approximation of the finite difference schemes in the boundary areas

The space of the one-dimensional pipeline is discretized with I sampling points, where the points with the indices $i = 1$ and $i = I$ represent the input and the output of the pipeline, respectively. Similarly, the calculation is performed for the points in time with the indexes $n = 1$ to $n = N$. By specifying the initial condition $T(x, t = 0)$, the temperature values T_i^1 for the entire pipeline is given. In addition, the input temperature values $T(x = 0, t)$ defined by T_1^n are given for all N points in time. In the following, the full implicit scheme and the Crank–Nicolson scheme, both FD approaches, are compared quantitatively to the NM. The implicit upwind scheme is not considered due to the lower accuracy expected from the lower numerical order of the scheme. For the creation of a determined set of equations, it is necessary to change the FD scheme of the two FD approaches at the discrete nodes at the end of the pipeline T_I^n . Here the implicit upwind scheme can be used, and is implemented in this work.

3. Test setup and simulation

The central idea of the quantitative results obtained in this work is to compare the simulated outlet temperatures of a pipeline, incorporating the effects of the steel core, with the measured data from [29]. The error metric typically used in this case is the Root Mean Square Error (RMSE) which has the advantage of over proportionally weighting outliers, which can create large deviations due to the possible consecutive faults arising from the simulation over several subsequent pipelines. The test setup used to produce the measurement data is described in detail and relevant parameters are given in [29]. The mass flow ranges from 0.1 m/s to 1.03 m/s, the temperature of the water is measured at the in- and output of the pipeline. The measured time series are available online [29]. These were created for four different scenarios, with input temperature differences ranging from 18 °C to 35 °C applied over periods ranging from 50 s to 7000 s [29]. As the time steps of the measured data are not strictly equidistant, the simulated data was linearly interpolated to enable a reasonable comparison.

4. Results

This chapter states the main quantitative and qualitative results of the comparison of the NM and the full implicit and Crank–Nicolson FD approaches.

The main quantitative results coming from a comparison of all four scenarios are depicted in Fig. 2 and Table 1. Note that the spatial step size of the NM is fixed to 39 m, which is determined by the length of the regarded pipeline. Considering other spatial step sizes for the NM would require artificially dividing the simulated pipeline into multiple pipelines, which would obviously deviate from the considered setup. The NM shows the smallest average RMSE over all scenarios with a minimum of 0.507 °C for the smallest considered time step of 0.5 s. From Fig. 2 (a) it is cognizable that a further reduction of the time steps does not show a significant change, as e.g. the reduction from 4 s to 0.5 s only shows a reduction of the RMSE of 0.0176 °C. This is valuable information as it allows reducing the amount of optimization variables adequately without significantly increasing the deviation between the pipeline model and the measurements. Regarding the FD approaches in Fig. 2 (b) and (c), the expected

Table 1. RMSE values of all three numerical approaches.

RMSE [°C]	NM	Full implicit FD				Crank–Nicolson FD			
		Δx	Δx	Δx	Δx	Δx	Δx	Δx	Δx
$\Delta t \backslash \Delta x$	39 m	2.44 m	4.88 m	9.75 m	19.5 m	2.44 m	4.88 m	9.75 m	19.5 m
0.5 s	0.507	0.762	0.724	0.891	1.409	0.862	0.775	0.902	1.406
4 s	0.525	0.497	0.578	0.869	1.445	0.847	0.764	0.907	1.426
8 s	0.547	0.532	0.617	0.906	1.487	0.841	0.763	0.919	1.448
16 s	0.590	0.764	0.822	1.040	1.571	0.871	0.804	0.959	1.493
32 s	0.628	1.128	1.164	1.303	1.714	1.125	1.039	1.123	1.588
64 s	1.038	1.654	1.673	1.746	1.992	1.817	1.732	1.631	1.890

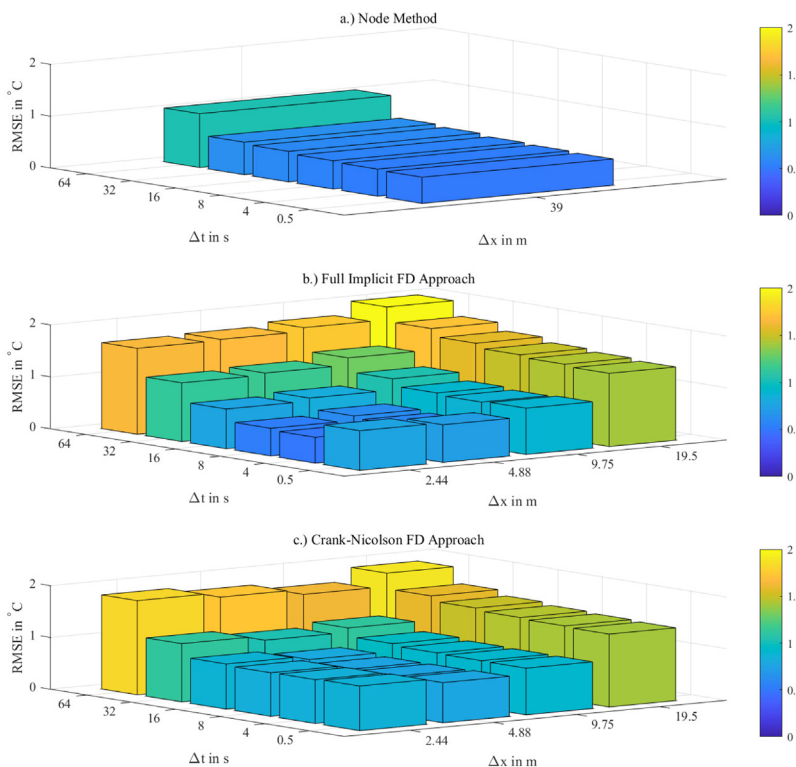


Fig. 2. RMSE of all three numerical approaches.

trend of small discretization steps in space and time leading to lower RMSEs can be observed for most of the $(\Delta x, \Delta t)$ -pairs, yielding minimal RMSEs of 0.497 °C at (2.44 m, 4 s) for the full implicit FD approach and 0.763 °C at (4.88 m, 8 s) for the Crank–Nicolson approach. Beyond these minima, the RMSEs increase for smaller discretization steps in place and time. This likely is an effect of the dispersive and dissipative errors which result from the numeric approximation of the PDE [28] and accumulate with every additional discretization point. Additionally, comparing the RMSE values over all $(\Delta x, \Delta t)$ -pairs in Table 1 of both FD approaches, it is evident that the full implicit approach has a lower mean RMSE of 0.643 °C. This results from less overshoot and oscillation.

For the qualitative comparison of the three approaches, the full implicit FD approach and the Crank–Nicolson FD approach can be grouped together, as their qualitative properties do not differ significantly. The only immediate difference lies in the fact that the full implicit FD approach only uses one sampling point in the current time step, while the Crank–Nicolson FD approach uses three. In comparison to the FD approaches, the NM requires a changing number of variables, strongly dependent on the current and previous mass flows, to calculate the output temperature of a pipeline. In the context of optimization problems, where a constant number of variables is desirable, this property of the FD approaches facilitates the implementation and reduces the computational burden compared with the NM. In addition, the discrete FD approaches do not need to approximate any integer auxiliary values,

circumventing an MINLP problem. Also, the FD approaches always maintain equidistant sampled information on the temperature of the medium in the pipeline. This equidistance of information can vary strongly with the NM, where the water masses with their respective temperatures are strongly dependent on the mass flows. Nevertheless, the NM has the advantage of not creating unwanted oscillations, arising from the dispersive and dissipative errors of the FD approaches [28]. Furthermore, while an NM approach for the case of varying mass flows has been presented in [30], this approach assumes that the mass flow direction does not change over the prediction horizon. A summary of the qualitative and quantitative comparison of the NM and the FD approaches is found in Table 2.

Table 2. Summary of the qualitative and quantitative comparison of the NM and the FD approaches.

Node method	Finite difference approaches
Solves the initial PDE with the MC	Solves the initial PDE by replacing the derivatives by various DQs
Higher implementational burden. Either high computational burden of MINLP or NLP approximation	Simple implementation
Changing number of optimization variables involved in calculation of outlet temperature of a pipeline	Constant number of optimization variables for calculation of the outlet temperature
Lowest mean RMSE due to less overshoot and oscillation	Dispersive and dissipative errors tend to grow with increasing discretization step sizes which result from the numeric approximation of the PDE
First differentiable approaches for varying mass flow directions exist	

5. Conclusion

The choice of an adequate pipeline model is a key challenge for DHN optimization tool designers as pipelines are the most numerous components in DHNs and both consecutive errors as well as the computational burden of the optimization problems can become large. In this work, several approaches for the modeling of DHN pipelines, based on solving the PDE for heat convection, were compared and their usability in the context of DHN optimization was described. Several valuable assumptions are stated which ease the computational burden while maintaining the necessary accuracy. A comparison of the different approaches with measurement data shows that the NM has the smallest computational error for most discretization steps and that it can be implemented for the case of varying mass flows. Still, the FD approaches, especially the implicit, unconditionally stable approaches, have properties that are advantageous in certain circumstances. These are the simplicity of their implementation, the constant number of variables required, and the constant information depth on the temperature fronts exhibited along the pipeline. Further research in the field of modeling DHN pipelines for varying mass flow directions in the application of operational optimization of DHNs is recommended as, until now, only very few approaches based on restrictive assumptions have been proposed. The qualitative and quantitative comparison presented in this paper, can help future DHN optimization tool designers to choose an adequate pipeline model.

Declaration of competing interest

The authors declare that they have no known competing financial interests or personal relationships that could have appeared to influence the work reported in this paper.

References

- [1] Gerhardt Norman, Sandau Fabian, Becker Sarah, Scholz Angela, Schumacher Patrick, Schmidt Dietrich. Heat transition 2030. 2017.
- [2] Lund H, Möller B, Mathiesen BV, Dyrelund A. The role of district heating in future renewable energy systems. *Energy* 2010;35:1381–90.
- [3] Yu Yanjuan, Chen Hongkun, Chen Lei, Chen Cheng, Wu Jun. Optimal operation of the combined heat and power system equipped with power-to-heat devices for the improvement of wind energy utilization. *Energy Sci Eng* 2019.
- [4] IEA. Technology collaboration programme on district heating and cooling including combined heat and power ANNEX XIII. 2020.
- [5] Zheng Jinfu, Zhou Zhigang, Zhao Jianing, Wang Jinda. Effects of the operation regulation modes of district heating system on an integrated heat and power dispatch system for wind power integration. *Appl Energy* 2018;1126–39.
- [6] Maurer J, Elsner C, Krebs S, Hohmann S. Combined optimization of district heating and electric power networks. *Energy Procedia* 2018;149:509–18.

- [7] Oppelt T, Urbaneck T, Gross U, Platzer B. Dynamic thermo-hydraulic model of district cooling networks. *Appl Therm Eng* 2016;102:336–45.
- [8] Liu X, Wu J, Jenkins N, Bagdanavicius A. Combined analysis of electricity and heat networks. *Appl Energy* 2016;162:1238–50.
- [9] Papageorgiou M. *Optimierung: statische, dynamische, stochastische verfahren für die anwendung*. Springer; 2015.
- [10] Bøhm B, Ha S-k, Kim W-t, Kim B-k, Koljonen T, Larsen HV, et al. Simple models for operational optimisation. 2002.
- [11] Li H, Sun Q, Zhang Q, Wallin F. A review of the pricing mechanisms for district heating systems. *Renew Sustain Energy Rev* 2015;42:56–65.
- [12] Nielsen MG, Morales JM, Zugno M, Pedersen TE, Madsen H. Economic valuation of heat pumps and electric boilers in the Danish energy system. *Appl Energy* 2016;167:189–200.
- [13] Duquette J, Rowe A, Wild P. Thermal performance of a steady state physical pipe model for simulating district heating grids with variable flow. *Appl Energy* 2016;178:383–93.
- [14] Oppelt T. *Modell zur auslegung und betriebsoptimierung von nah- und fernkältenetzen* (Ph.D. dissertation), Technische Universität Chemnitz; 2015.
- [15] Benonysson A. *Dynamic modelling and operational optimization of district heating systems*. (Ph.D. dissertation), Lyngby: Technical University of Denmark; 1991.
- [16] van der Heijde B, Aertgeerts A, Helsen L. Modelling steady-state thermal behaviour of double thermal network pipes. *Int J Therm Sci* 2017;117:316–27.
- [17] Grosswindhager S, Voigt A, Kozek M. Linear finite-difference schemes for energy transport in district heating networks. In: *Proceedings of the 2nd international conference on computer modelling and simulation*, 2011. pp. 35–42.
- [18] Pålsson H. *Methods for planning and operating decentralized combined heat and power plants*. (Ph.D. dissertation), Technical University of Denmark; 2000.
- [19] Wang Y, You S, Zhang H, Zheng X, Zheng W, Miao Q, et al. Thermal transient prediction of district heating pipeline: Optimal selection of the time and spatial steps for fast and accurate calculation. *Appl Energy* 2017;206:900–10.
- [20] Dénarié A, Aprile M, Motta M. Heat transmission over long pipes: New model for fast and accurate district heating simulations. *Energy* 2019;166:267–76.
- [21] Gabriellaitiene I, Sundén B, Kacianauskas R, Bohm B. Dynamic modeling of the thermal performance of district heating pipelines. In: *4th baltic heat transfer conference*, 2003. pp. 185–192.
- [22] Olsthoorn D, Haghighat F, Mirzaei PA. Integration of storage and renewable energy into district heating systems: A review of modelling and optimization. *Sol Energy* 2016;136:49–64.
- [23] Talebi B, Mirzaei PA, Bastani A, Haghighat F. A review of district heating systems: modeling and optimization. *Front Built Environ* 2016;2:22.
- [24] Ortega J, Bruno JC, Coronas A, Grossman IE. Review of optimization models for the design of polygeneration systems in district heating and cooling networks. *Comput Aided Chem Eng* 2007;2007:1121–6.
- [25] Polifke W, Kopitz J. *Wärmeübertragung: Grundlagen, analytische und numerische Methoden*. München: Pearson Studium; 2009.
- [26] Sarra SA. The method of characteristics with applications to conservation laws. *J Online Math Appl* 2003;3:1–16.
- [27] Tschuch N. *Implementation of a market based model predictive control approach for coupled electric power and district heating networks*. (B.Sc. Thesis (German)), Karlsruhe Institute of Technology; 2019.
- [28] Munz C-D. *Numerische Behandlung gewöhnlicher und partieller Differenzialgleichungen: Ein Anwendungsorientiertes Lehrbuch für Ingenieure*. 4th ed. Berlin, Heidelberg: Springer Berlin Heidelberg; 2019.
- [29] van der Heijde B, Fuchs M, Tugores CR, Schweiger G, Sartor K, Basciotti D, et al. Dynamic equation-based thermo-hydraulic pipe model for district heating and cooling systems. *Energy Convers Manage* 2017;151:158–69.
- [30] Tröster S. *Zur betriebsoptimierung in kraft-wärme-kopplungssystemen unter berücksichtigung der speicherfähigkeit des fernwärmenetzes*. Fraunhofer-IRB-Verlag; 1999.